

Spin-0 soliton formation in spin-Peierls systems: Charge-transfer complexes DAP-TCNQ and DAP-DMTCNQ

Taro Sekikawa

*Institute for Molecular Science, Okazaki 444, Japan
and Department of Physics, University of Tokyo, Tokyo 113, Japan*

Hiroshi Okamoto

Research Institute for Science Measurements, Tohoku University, Sendai 980, Japan

Tadaoki Mitani

Japan Advanced Institute of Science and Technology, Ishikawa 923-12, Japan

Tamotsu Inabe

Department of Chemistry, Hokkaido University, Sapporo 060, Japan

Yusei Maruyama

Department of Materials Chemistry, Hosei University, Koganei, Tokyo 184, Japan

Takayoshi Kobayashi*

Department of Physics, University of Tokyo, Tokyo 113, Japan

(Received 11 April 1996; revised manuscript received 10 October 1996)

The optical and magnetic properties of the spin-Peierls system, segregated-stack charge-transfer complexes, 1,6-pyrenediamine (DAP)-tetracyanoquinodimethane (TCNQ) and DAP-2,5-dimethyl-TCNQ (DMTCNQ), are investigated to gain insight into the nonlinear excitations in the spin-Peierls system. The band filling of the system slightly deviates from the half-filled regime and the lattice is dimerized along the chain. In the optical reflectance spectra, a midgap band below the Hubbard band is found. By referring to the magnetic properties, the midgap band is ascribed to a spin-0 soliton formed by a spinless domain wall between the twofold degenerate ground states of the dimerized chain. The amplitude of dimerization is modified by the interchain hydrogen bond. [S0163-1829(97)05308-3]

I. INTRODUCTION

Solitons in the one-dimensional (1D) half-filled system with twofold degenerate ground states have been shown to be indispensable for understanding the optical and magnetic properties as well as the transport properties of the 1D system.¹ The 1D system investigated so far from a viewpoint of nonlinear excitations is the Peierls system, where the electron-phonon interaction is dominant in comparison with the electron-electron Coulomb correlation. However, the spin-Peierls system, in which the electron-electron Coulomb repulsion plays an essential role in the electronic properties of the system, also has twofold degenerate ground states, *A* and *B* phases schematically depicted in Fig. 1(a) for the strong limit of the electron localization.² The $S = \frac{1}{2}$ spin of the localized electron aligns antiferromagnetically. The 1D lattice is distorted to form the spin singlet pair because of the spin-lattice interaction.

The domain walls between *A* and *B* phases are also expected to behave as kink-type defects or solitons in the spin-Peierls system. In fact the spin-0 and spin solitons, which are schematically illustrated in Figs. 1(b) and 1(c), are theoretically shown to be relevant excitations in the spin-Peierls system.³ Furthermore the polaron configuration [Fig. 1(d)] might also exist, in which the lattice dimerization is inter-

rupted or weakened because of neutral sites in the chain. However, such nonlinear excitations in the spin-Peierls system have been scarcely investigated experimentally. It is therefore interesting to study the nonlinear excitations in the spin-Peierls system.

In the present study, 1,6-pyrenediamine (DAP)-tetracyanoquinodimethane (TCNQ) (Ref. 4) is chosen as a model material to investigate nonlinear excitations in the spin-Peierls system. It is a quasi-1D charge-transfer (CT) complex composed of two segregated columns, DAP and TCNQ. The structural analysis and the transport properties suggest that the complex belongs to the Mott-Hubbard system, where the electron-electron Coulomb repulsion energy is dominant compared with the electron-transfer energy.⁴ In addition, in the present work, the lattice of DAP-TCNQ will be shown to be dimerized along the stacking axis, leading to the conclusion that the complex is a spin-Peierls system together with both the optical and magnetic properties. In DAP-TCNQ the degree of charge transfer from DAP to TCNQ is fractional and close to unity, indicating that there are neutral sites in the 1D chain, i.e., the band filling slightly deviates from the half-filled regime.⁴ The fractional band filling of DAP-TCNQ corresponds to the introduction of carriers in the half-filled 1D chain. The carrier effect is expected to identify nonlinear excitations in the spin-Peierls system as

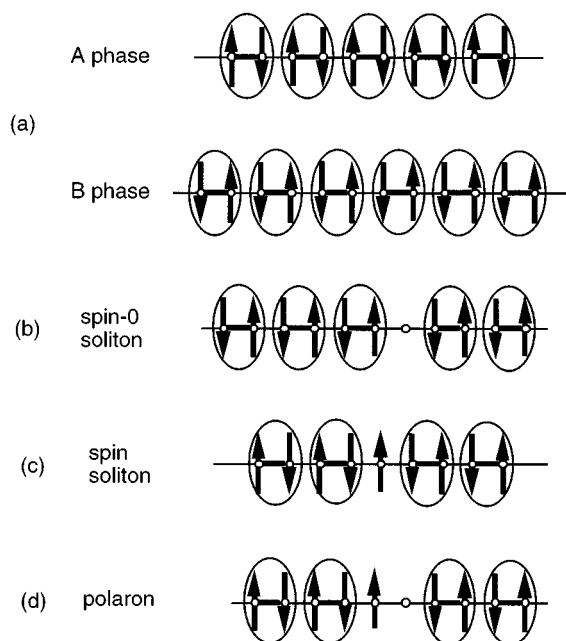


FIG. 1. Schematic structure of the (nearly) half-filled 1D chain of the spin-Peierls system. The arrow indicates an electron and its spin state. Spins align antiferromagnetically. Ovals represent the spin singlet pair with the lattice dimerization. (a) Two phases of the dimerized chains, A and B phases, (b) spin-0 soliton, (c) spin soliton, and (d) polaron.

investigated in the Peierls system.¹ Therefore DAP-TCNQ provides a unique opportunity to study nonlinear excitations in the spin-Peierls system.

In addition to these features, the hydrogen bond is formed between the DAP and TCNQ column.⁴ It was found that the interchain hydrogen-bond affects the soliton excitation in the halogen-bridged mixed-valent metal (MX) compounds, which is the Peierls system.^{5,6} It is also interesting to investigate the effect of the interchain hydrogen bond on the spin-Peierls state.

Motivated by these expectations, we report the results of the polarized reflectance spectrum and ESR measurements of DAP-TCNQ after summarizing the crystal structure and the transport properties. Optical measurements are suitable to probe both the electronic and the conformational structures of DAP-TCNQ. The polarized reflectance spectrum from the visible to mid-IR region reveals a midgap band below the Hubbard gap. The origin of the midgap band is discussed with the result of the temperature dependence of ESR measurements. Furthermore the optical and magnetic properties of DAP-2,5-dimethyl-TCNQ (DMTCNQ) were investigated to compare with DAP-TCNQ.

II. CRYSTAL STRUCTURE AND TRANSPORT PROPERTIES OF DAP-TCNQ

For the sake of the later discussion, the crystal structure and transport properties of DAP-TCNQ reported in Ref. 4 are briefly summarized in this section.

DAP and TCNQ stack in a segregated manner along the c axis in a crystal with the uniform intermolecular distance as shown in Fig. 2. A DAP-TCNQ crystal has a triclinic struc-

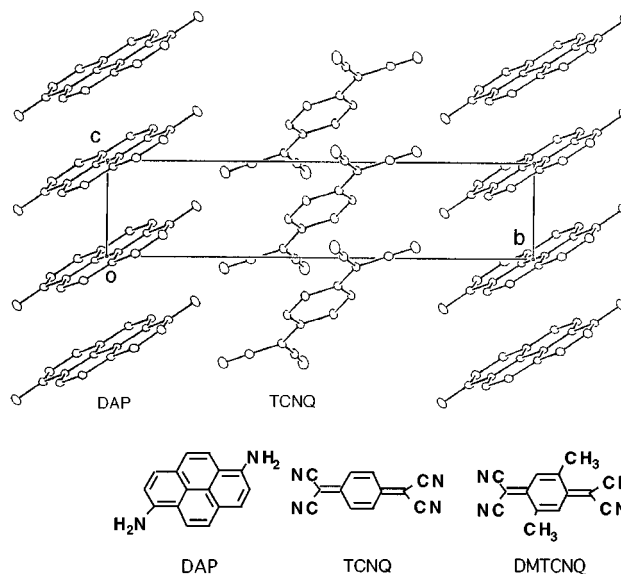


FIG. 2. Crystal structure of DAP-TCNQ and the constitutional formulas of DAP, TCNQ, and DMTCNQ molecules. The molecules are stacked segregatededly along the c axis (Ref. 4).

ture, belonging to the space group $P\bar{1}$. The lattice parameter is listed in Table I. The distortion along the stacking axis was not observed. The refined anisotropic thermal parameters are normal and the final R values are quite reasonable with the structure analyzed based on the uniform stacking. One of crystallographic features of the DAP-TCNQ crystal is that TCNQ and DAP are connected with two kinds of N-H \cdots N hydrogen bonds to form the hydrogen-bonded network along the (0,3,1) plane; the hydrogen-bond lengths are 2.980 and 3.020 Å at 295 K, which are shorter than the van der Waals radius of a nitrogen atom (3.2 Å).

One of the fundamental parameters that characterize the electronic properties of a CT complex is the degree of charge transfer from a donor to an acceptor molecule (ρ), i.e., band filling in a crystalline phase. From the empirical relation between ρ and the bond length of the TCNQ molecule proposed by Kistenmacher *et al.*,⁷ the charge transfer from DAP to TCNQ is estimated as 0.96 at 295 K, suggesting that the band filling slightly deviates from the half-filled regime.

Since π orbitals in the columns of DAP and TCNQ overlap efficiently along two parallel stack axes because of the short intermolecular distance of 3.25 Å in each column, the complex has quasi-1D electronic properties. In fact, the electric conductivity is anisotropic. Its parallel component to the stacking axis increases with temperature, i.e., it is semicon-

TABLE I. Lattice parameters.

	DAP-TCNQ ^a	DAP-DMTCNQ
a (Å)	7.937(1)	8.213(1)
b (Å)	17.307(3)	18.725(3)
c (Å)	3.898(1)	3.594(6)
α (deg)	90.38(2)	100.82(6)
β (deg)	93.82(2)	90.25(5)
γ (deg)	109.77(1)	112.16(2)

^aReference 4.

ductive. The activation energy of the conductivity along the c axis is 0.26 eV. No metal-to-insulator transitions are observed between 77 and 400 K. These two results suggest that the complex belongs to the Mott-Hubbard system, where the electron-electron Coulomb repulsion energy is dominant compared with the electron-transfer energy. The temperature dependence of the thermoelectric power (TEP) also suggests that DAP-TCNQ is a semiconductor. The TEP value between 230 and 300 K is nearly independent of temperature, while TEP of a metallic CT complex has a linear relation with temperature.^{8,9}

III. EXPERIMENT

Single crystals of the CT complexes DAP-TCNQ and DAP-DMTCNQ were prepared using the cosublimation method. DAP and TCNQ (DMTCNQ) were placed on opposite sides of the glass tube evacuated at about 10^{-3} Torr. The temperatures of DAP and TCNQ (DMTCNQ) were kept around 170 and 150 °C, respectively, for approximately three days. The grown crystals of DAP-TCNQ and DAP-DMTCNQ have the form of dark purple plates with maximum sizes of about $0.8 \times 0.5 \times 0.08$ and $0.2 \times 0.1 \times 0.08$ mm³, respectively. The plate surface of the DAP-TCNQ crystal is parallel to the ac plane. The powder diffraction pattern of DAP-DMTCNQ was used to investigate the crystal structure, because it was very difficult to obtain large enough crystals of DAP-DMTCNQ for x-ray structural analysis.

The Raman spectrum was measured with a Nd:YLF laser, a charge-coupled device camera, and a monochromator to estimate the degree of charge transfer. ESR was measured at various temperatures between 10 and 300 K using a 2-mg sample composed of many single crystals sealed in a quartz tube with He gas with a standard ESR X-band spectrometer. For the measurement of the polarized reflectance spectrum, a microscope with a Cassegrain mirror was used to condense the light, since the sample was too small to be measured by the usual method. For both the visible and near-IR regions, light from a halogen incandescent lamp was focused on a sample by a microscope after passing through a monochromator and a polarizer. The reflected light was detected with a photomultiplier in the visible region and with a PbS cell detector in the near-IR region. For the mid-IR region, the Fourier-transform infrared (FTIR) spectrometer was used. Light from the FTIR spectrometer was also focused on the sample by the microscope and detected with a Hg_xCd_{1-x}Te detector. A single crystal for the measurement of the reflectance spectrum was mounted on a goniometer cooled by a cold finger tip in He gas-flow-type cryostat with BaF₂ windows. The temperature was measured using a AuFe-chromel thermocouple attached close to the sample.

IV. RESULTS

A. X-ray diffraction pattern of DAP-DMTCNQ

Figure 3 shows the x-ray powder diffraction patterns of DAP-TCNQ and DAP-DMTCNQ. Since the structure of DAP-TCNQ is known,⁴ the calculated diffraction profile was used to determine the indices of the Bragg reflections in Fig. 3. The diffraction pattern of DAP-DMTCNQ is similar to that of DAP-TCNQ, suggesting that the crystal structure of

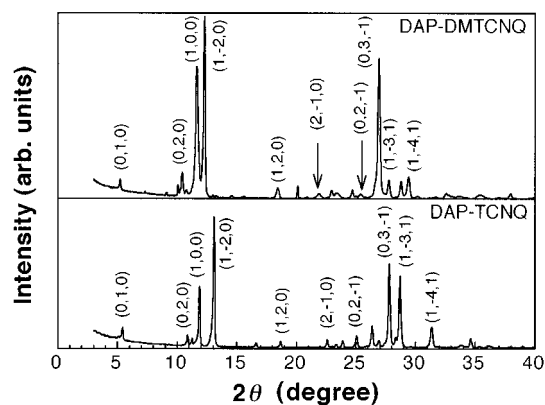


FIG. 3. X-ray diffraction patterns of DAP-TCNQ and DAP-DMTCNQ. The numbers indicate the indices of the Bragg reflection.

DAP-DMTCNQ is similar to that of DAP-TCNQ. The Bragg reflection indices are given at the peaks in Fig. 3. Using these indices, the lattice parameters of DAP-DMTCNQ are calculated as in Table I, indicating the unit cell is sheared to some extent along the stacking axis from that of the TCNQ complex.

B. Estimation of the degree of charge transfer

It is important to evaluate the degree of charge transfer in the CT complexes, since the electronic properties are sensitive to ρ .^{10,11} In the case of $\rho=1$, each of two neighboring molecules already has an unpaired electron and the energy to activate conduction involves large electron-repulsion energy. Such a complex is an insulator and is called a Mott insulator. For $\rho<1$, an unpaired electron has the chance of finding a neutral neighboring molecule and the electron can move in the stack without suffering from the large Coulomb repulsion. Such a complex is in a metallic state.

The degree of charge transfer of DAP-TCNQ has been estimated as 0.96 by x-ray structural analysis.⁴ Another independent way to estimate ρ is by vibrational spectroscopy. There is an empirical linear relation between the frequency of the Raman active C=C stretching mode in TCNQ and ρ .¹² Since the frequency of the C=C stretching mode of DAP-TCNQ was 1401 ± 1 cm⁻¹, ρ is estimated to be 0.90 ± 0.02 . Taking account of the accuracy of the empirical rules, this value is almost in agreement with the result estimated by x-ray structural analysis and indicates that there exist neutral sites in the 1D chain; namely, the band filling deviates from the half-filled regime. Although it is difficult to discuss the density of the neutral site from these experimental results in detail, it is conjectured that ρ would be close to unity: If DAP-TCNQ has ρ close to 0.8, it would belong to the Peierls system and be metallic at room temperature. It is necessary to measure ρ by some other methods, e.g., diffused x-ray scattering, to determine the value more accurately.

In the case of DAP-DMTCNQ, such a relation is not known. However, ρ appears to be the same, since the frequency of the IR-active C≡N stretching b_{1u} mode of DMTCNQ—which is also sensitive to ρ (Ref. 13)—was the

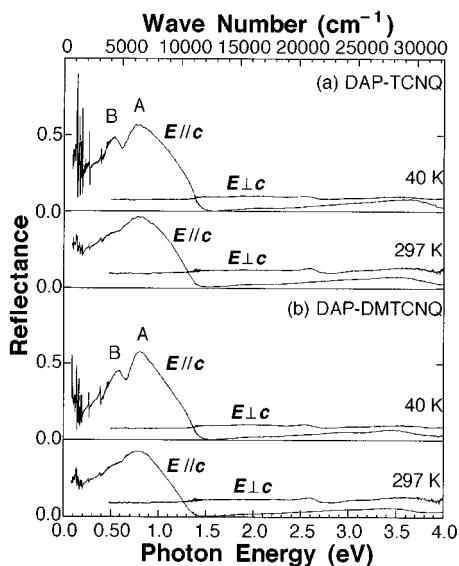


FIG. 4. Optical reflectance spectra of (a) DAP-TCNQ and (b) DAP-DMTCNQ at 40 and 297 K. Light polarizations (\mathbf{E}) were parallel (\parallel) and perpendicular (\perp) to the stacking axis (c axis). The A band is the CT band. The B band grows at low temperature.

same as that of DAP-TCNQ. This estimation of ρ is consistent with the interpretation of all the experimental results of the present study.

C. Reflectance spectrum

1. Visible and near-IR regions

The reflectance spectra with polarizations parallel and perpendicular to the stacking axis (c axis) of DAP-TCNQ and DAP-DMTCNQ at 40 and 297 K are shown in Figs. 4(a) and 4(b), respectively. The reflectance spectrum with a perpendicular polarization below 0.3 eV could not be measured with a good signal-to-noise ratio. A strong reflectance band (A) between 1.2 and 0.6 eV with a polarization parallel to the c axis was observed in each complex, while no prominent structures were observed with a perpendicular polarization. The similarity of the reflectance spectra between these complexes also suggests the 1D crystal structure of DAP-DMTCNQ, which is consistent with the x-ray powder diffraction pattern.

The A band is assigned to the CT transition band, corresponding to the following charge-transfer process along the stacking axis: $\text{TCNQ}^- + \text{TCNQ}^- \rightarrow \text{TCNQ}^0 + \text{TCNQ}^{2-}$ ($\text{DMTCNQ}^- + \text{DMTCNQ}^- \rightarrow \text{DMTCNQ}^0 + \text{DMTCNQ}^{2-}$) and $\text{DAP}^+ + \text{DAP}^+ \rightarrow \text{DAP}^0 + \text{DAP}^{2+}$; the energy required for the CT transition approximately corresponds to the on-site electron Coulomb repulsion energy (U). The value of U has been estimated to be about 1.1 eV in the TCNQ column from the peak energy of the CT band of potassium salt of TCNQ (K-TCNQ), which is a half-filled system.^{14–17} The peak energy of the A band is close to the CT transition energy. On the other hand, U of DAP is not known. However, since only one reflectance structure was observed at room temperature, the U of the DAP column is considered to be close to that of the TCNQ column. The observation of the CT band indicates that the Hubbard gap is opened due to the

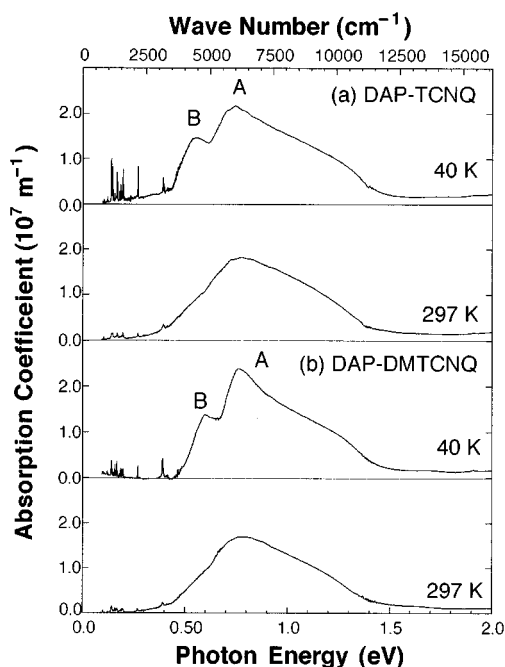


FIG. 5. Absorption spectra of (a) DAP-TCNQ and (b) DAP-DMTCNQ obtained by the Kramers-Kronig transformation of the reflectance spectra at 40 and 297 K. The A and B bands are the CT and midgap bands, respectively.

electron-electron interaction in both DAP-TCNQ and DAP-DMTCNQ.

A remarkable change in the reflectance spectra at low temperatures is that the B band at 0.5 eV below the CT band grows with decreasing temperature in both complexes. The B band is clearly visible in Fig. 4 at 40 K. Figures 5(a) and 5(b) show the absorption spectra of DAP-TCNQ and DAP-DMTCNQ, respectively, at 40 and 297 K. These spectra were obtained using the Kramers-Kronig transformation of the reflectance spectra with the assumption of a constant reflectance below 0.1 eV and the ω^{-4} law above 4 eV, where ω is the optical frequency. The B band in the reflectance spectrum corresponds to the midgap band below the Hubbard gap. The temperature dependence of the intensities of the CT and midgap bands of DAP-TCNQ and DAP-DMTCNQ are estimated by integrating the band spectrum over the probed

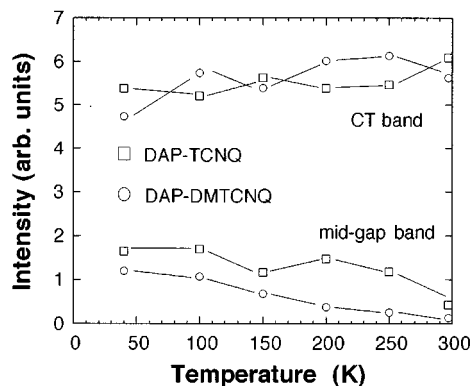


FIG. 6. Temperature dependence of the intensities of the CT and midgap transitions. The solid lines are to guide the eye.

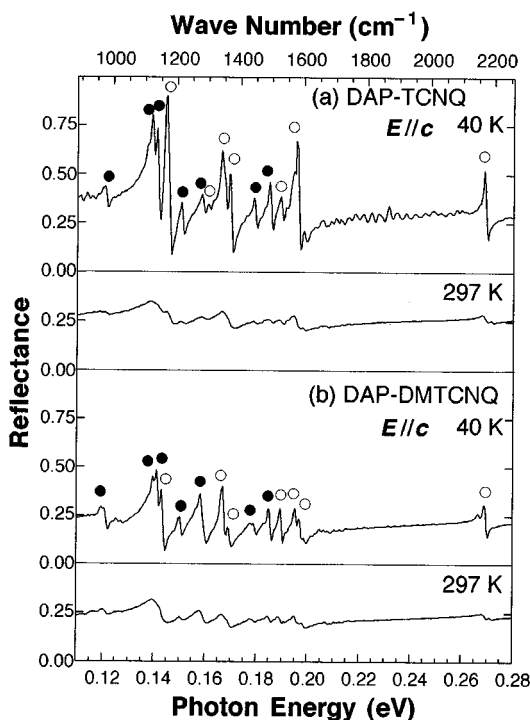


FIG. 7. Reflectance spectra of (a) DAP-TCNQ and (b) DAP-DMTCNQ at 40 and 297 K in the mid-IR region with a polarization parallel to the stacking axis ($E\parallel c$). (a) Open circles and closed circles represent the activated a_g modes of TCNQ and DAP, respectively. (b) Open circles and closed circles represent the a_g modes of DMTCNQ and DAP, respectively.

photon energy numerically and are shown in Fig. 6. The intensity of the midgap band of DAP-DMTCNQ was smaller than that of DAP-TCNQ at every temperature. The origin of the B band will be discussed in Sec. V B.

2. Mid-IR region

The wide spectral range reflectance spectra enables us to obtain information not only on the electronic structure but also on the conformational structure. In particular, the IR activation of the intramolecular a_g -mode vibration due to the electron-intramolecular vibration (emv) coupling is a sensitive probe for the conformational changes of the 1D CT complexes.^{18–20} Considerable efforts have been made on the studies of specific totally symmetric intramolecular vibrations in various segregated-stack crystals^{14,17,21–27} and mixed-stack crystals.^{28–30} The induced dipole moment of the a_g mode is parallel to the stacking axis and its magnitude strongly depends on the amplitude of the emv coupling and on the difference in the intradimer and interdimer electron-transfer interactions, which is supposed to be nearly proportional to the dimeric molecular displacement in the case of weak dimerization.¹⁷ The activation of the a_g mode, with a polarization parallel to the stacking axis, is direct evidence of the lattice distortion.

For the purpose of detecting the lattice distortion, the polarized reflectance spectra of DAP-TCNQ and DAP-DMTCNQ were measured at various temperatures in the mid-IR region. The spectra of DAP-TCNQ and DAP-DMTCNQ with a polarization parallel to the stacking axis

TABLE II. (a) Frequencies (cm^{-1}) of the activated a_g modes of TCNQ and DMTCNQ. (b) Frequencies (cm^{-1}) of the IR activated a_g modes of DAP.

Sample	Molecule	Frequency	Frequency in K-TCNQ ^a
DAP-TCNQ	TCNQ	2167	2175
		1579	1571
		1525	1508
		1368	1365
		1341	1330
		1298	1320
DAP-DMTCNQ	DMTCNQ	1164	1174
		2168	
		1586	
		1574	
		1529	
		1365	
		1345	
		1153	
		Frequency in DAP-TCNQ	Frequency in DAP-DMTCNQ
		1492	1491
		1441	1439
		1278	1275
		1214	1212
		1137	1140
		1121	1126
		970	968

^aReference 11.

($E\parallel c$) at 40 and 297 K are shown in Figs. 7(a) and 7(b), respectively. The strong activation of the a_g modes is clearly seen from the figures, indicating the lattice distortion along the stacking axis at low temperatures. Since DAP-TCNQ is a complex of DAP and TCNQ, the activated modes can be attributed to the component molecules. The frequencies of the activated a_g modes of the TCNQ molecule in K-TCNQ have been determined as shown in Table II.¹⁴ Since ρ of DAP-TCNQ is close to 1, the a_g modes of the TCNQ molecule are expected to be almost the same as those of K-TCNQ. Hence the activated modes of DAP-TCNQ can be assigned as shown in Fig. 7(a), with open circles for the TCNQ molecule and closed circles for the DAP molecule. The frequencies of the a_g modes of TCNQ and DAP are listed in Tables II(a) and II(b), respectively. In the case of DAP-DMTCNQ, the observed activation of the symmetric modes is shown in Fig. 7(b), indicating the lattice distortion. Since the a_g modes of the DAP molecule are identified, those of the DMTCNQ molecule can be assigned as shown in Fig. 7(b) (open circles for DMTCNQ and closed circles for DAP). The frequencies of them are listed in Tables II(a) and II(b), respectively. It is noteworthy that both the DAP and TCNQ (DMTCNQ) columns have been already dimerized even at 297 K, which is shown by the observation of the a_g modes at 297 K.

Figure 8 shows the temperature dependence of the intensities (S) of the a_g modes, whose frequencies are 2167 cm^{-1}

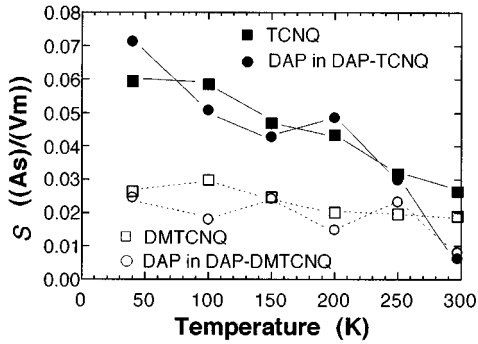


FIG. 8. Temperature dependence of the intensities of the activated a_g modes: Closed circles and squares represent the modes of 2167 cm^{-1} of TCNQ and 1214 cm^{-1} of DAP in DAP-TCNQ, respectively. Open circles and squares represent the modes of 2168 cm^{-1} of DMTCNQ and 1212 cm^{-1} of DAP in DAP-DMTCNQ, respectively. The solid and dashed lines are to guide the eye.

of TCNQ and 1214 cm^{-1} of DAP in DAP-TCNQ and 2168 cm^{-1} of DMTCNQ and 1212 cm^{-1} of DAP in DAP-DMTCNQ. The intensity of the mode S is defined by assuming the following complex dielectric constant as a function of the frequency ω :

$$\varepsilon(\omega) = \varepsilon_\infty + \frac{S\omega_0^2}{\omega_0^2 - \omega^2 - i\Gamma\omega}, \quad (1)$$

where ω_0 is the resonance frequency and Γ is the width of an a_g mode, ε_∞ is a constant value contributed by the background polarization. The value of S is estimated by fitting the reflectance spectrum by the least-square method to the reflectance $R(\omega)$ defined as

$$R(\omega) = \frac{1 + |\varepsilon| - \sqrt{2(|\varepsilon| + \varepsilon_1)}}{1 + |\varepsilon| + \sqrt{2(|\varepsilon| + \varepsilon_1)}}, \quad (2)$$

where ε_1 is the real part of $\varepsilon(\omega)$. The estimated values of S of TCNQ, for example, are 0.059 and 0.026 and those of DMTCNQ are 0.026 and 0.019 at 40 and 296 K, respectively. Because S increases with decreasing temperature as shown in Fig. 8, the amplitudes of lattice distortions of both the DAP and TCNQ (or DMTCNQ) columns are enhanced along the stacking axis at lower temperature. In addition, Fig. 8 shows that the amplitude of distortion in the DAP-TCNQ column is always larger than that in DAP-DMTCNQ in the range of the experimental temperature.

Other important information is obtained from the IR spectroscopy. The strength of the hydrogen bond can be compared between the DAP-TCNQ and DAP-DMTCNQ from the frequency shift of the N-H stretching mode of the DAP in the complexes. Figure 9 shows the IR absorption spectra of DAP molecules, DAP-TCNQ, and DAP-DMTCNQ. Two absorption bands were observed in each complex around 3330 and 3180 cm^{-1} and they are assigned to the N-H stretching modes. Since the structural analysis indicates that two different hydrogen bonds in length are formed between the DAP and TCNQ column,⁴ two N-H stretching modes are expected. Thus the mode observed around 3180 cm^{-1} is considered to be shifted to lower frequency due to the hydrogen bond. The frequencies of the shifted N-H stretching modes

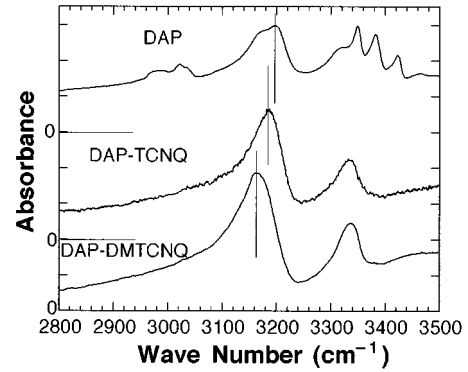


FIG. 9. Absorption spectra of the N-H stretching vibrations (vertical lines) of DAP molecules, DAP-TCNQ, and DAP-DMTCNQ.

of the DAP molecules, DAP-TCNQ and DAP-DMTCNQ, were 3194 , 3185 , and 3165 cm^{-1} , respectively, indicated by the vertical lines in Fig. 9. The strength of the hydrogen bond in DAP-DMTCNQ is stronger than that in DAP-TCNQ, because the frequency shift in DAP-DMTCNQ, 29 cm^{-1} , is larger than that of DAP-TCNQ, 9 cm^{-1} . However, the hydrogen bond does not appear to be strong enough to order the dimerization phase two dimensionally, because the frequency shift in the present system is much smaller than that of the MX compound, 430 cm^{-1} ,³¹ in which the phase of the charge density wave is correlated two dimensionally.^{5,6} The relatively small frequency shifts in the present CT complexes are consistent with no interchain correlation of the dimerization phase suggested by x-ray structural analysis.⁴

D. Spin susceptibility

In order to obtain information on the spin states of DAP-TCNQ and DAP-DMTCNQ, the temperature dependence of ESR was measured. Figure 10(a) shows the temperature de-

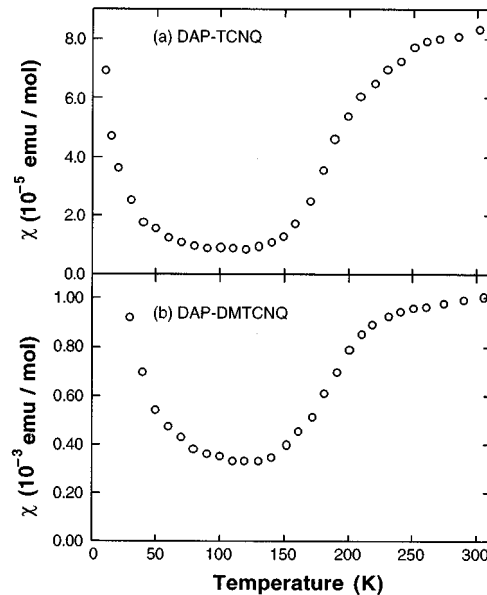


FIG. 10. Temperature dependence of the spin susceptibilities χ of (a) DAP-TCNQ and (b) DAP-DMTCNQ.

pendence of the spin susceptibility of DAP-TCNQ. It decreases to 1.0×10^{-5} emu/mol with temperature from 300 to 100 K and then rapidly increases at lower temperatures. The latter dependence follows the Curie law. Similar temperature dependence was observed in the case of DAP-DMTCNQ as shown in Fig. 10(b). The residual spin densities below 100 K of DAP-TCNQ and DAP-DMTCNQ are estimated to be 9.2×10^{-4} and 3.7×10^{-2} per one site, respectively, using the Curie law. The Curie contribution could arise from either interruptions in the stacks or spins localized by impurities. The spin density of DAP-DMTCNQ below 100 K was larger than that of DAP-TCNQ. This is probably due to the poorer quality of the sample, since the sample crystals of DAP-DMTCNQ grown were much smaller than that of DAP-TCNQ.

V. DISCUSSION

A. DAP-TCNQ and DAP-DMTCNQ as the spin-Peierls systems

The essential difference between the spin-Peierls and the Peierls system in the half-filled state is the ratio of U to the electron-transfer energy (t), resulting in the different optical, magnetic, and transport properties.² The material of the spin-Peierls system is an insulator and the magnetic susceptibility reduces to zero as a function of temperature with lattice dimerization.

The following four experimental results suggest that DAP-TCNQ belongs to the spin-Peierls system, even though the band filling deviates from the half-filled regime. (i) The temperature dependence of the electric conductivity along the stacking axis does not show metal-to-insulator transitions between about 150 and 400 K and is always semiconducting with the activation energy 0.26 eV.⁴ (ii) The reflectance spectrum along the stacking axis shows the large reflectance due to the CT transition with a peak around 0.8 eV. [Fig. 4(a)]. (iii) The a_g modes of intramolecular vibrations are activated with the polarization parallel to the c axis in the IR reflectance spectrum as shown in Fig. 7(a), although the a_g modes should be IR inactive in the uniform stack. (iv) The spin susceptibility rapidly decreases to less than 1×10^{-5} emu/mol with temperature from 300 to 100 K as shown in Fig. 10(a).

The experimental results (i) and (ii) can be explained by the following two mechanisms. One is that the Peierls transition has already taken place even at 400 K and hence the observed energy gap is the Peierls gap. The other is that DAP-TCNQ is a Mott insulator and the energy gap corresponds to the Hubbard gap. However, the first mechanism is ruled out for the following reason: If the DAP-TCNQ is the Peierls system with the large gap energy 0.8 eV, the lattice should be distorted largely enough to be observed by the x-ray structural analysis in order to open the large energy gap. However, the lattice distortion was small and was detected only by the IR spectroscopy, which is the sensitive probe into the lattice distortion.¹⁷ In addition to that, the Peierls gaps observed so far are less than 0.5 eV, which is smaller than that of the present system.¹⁰ On the other hand, the gap energy is consistent with those of the CT bands in K-TCNQ and Rb-TCNQ, in which the CT bands were observed even above the temperature of the phase transition.¹⁷ Thus DAP-TCNQ is considered to be a Mott insulator.

The experimental result (iii) indicates the lattice distortion along the stacking axis (c axis) as mentioned in Sec. IV C. From the results, (iii) and (iv), the rapid decrease in the spin susceptibility in accord with the activation of the a_g mode between 150 and 200 K is interpreted as the decrease in the spin-triplet state thermally populated and the formation of the spin-singlet pair with the lattice dimerization. Consequently, from these four experimental results, DAP-TCNQ is identified as the spin-Peierls system.

The transition temperature to the spin-Peierls state would be above 297 K, since the lattice has already been dimerized at 297 K taking account of the activation of the a_g modes at 297 K. Even after the phase transition, the amplitude of the dimerization becomes larger with a decrease in temperature suggested from the temperature dependence of the a_g modes. Therefore the spin gap becomes larger with decreasing in temperature, which was also observed in K-TCNQ.³² The rapid decrease in the spin susceptibility from 300 to 100 K is not only due to the decrease in the thermally populated triplet state but is also due to the larger spin gap with temperature.

Generally the transition temperature of the typical spin-Peierls system is much lower than room temperature. However, that of DAP-TCNQ is much higher than the typical transition temperature. This is considered to be due to the relatively larger electron-transfer energy compared with the Coulomb-repulsion energy. In that sense DAP-TCNQ is the intermediate case between the regular Peierls system and the spin-Peierls system. However, the gap energy is determined not by the lattice distortion but by the electron correlation. Thus DAP-TCNQ is classified into the spin-Peierls system in the present paper.

The obtained crystals of DAP-DMTCNQ were too small for the measurement of the temperature dependence of the electric conductivity. However, the other properties were similar to DAP-TCNQ as shown in Figs. 4(b), 7(b), and 10(b). Hence DAP-DMTCNQ is also considered to be the spin-Peierls system.

B. Midgap state in the spin-Peierls system

In the absorption spectra of DAP-TCNQ and DAP-DMTCNQ, the B bands appear below the CT bands with a decrease in temperature as shown in Fig. 4 at 40 K. On the other hand, no new bands appear when the light polarization is perpendicular to the stacking axis. The anisotropy of the midgap band indicates that the midgap band is related to the 1D excitation along the stacking axis.

The carrier effect on the optical spectrum of the spin-Peierls system is still an experimentally unresolved problem. The investigation of the optical properties of DAP-TCNQ and DAP-DMTCNQ is expected to reveal nonlinear excitations in the spin-Peierls system. The difference between DAP-TCNQ and K-TCNQ, although both complexes are identified as spin-Peierls systems,³²⁻³⁴ is the degree of charge transfer: K-TCNQ is the half-filled system, while the band filling of DAP-TCNQ deviates from the half-filled regime. Thus the origin of the midgap band appears to be neutral sites in the 1D chain, since no midgap bands have been observed in K-TCNQ at low temperature.¹⁴⁻¹⁷

The presence of the neutral sites is expected to lead to the new transition band corresponding to the electron transfer

from the second nearest to the nearest neighbor of the neutral site in the extended Hubbard model,³⁵ which includes the Coulomb repulsion energy between the nearest-neighbor sites (V). The transition energy is smaller than the CT transition energy by V . In the case of TCNQ columns, V is estimated to be about 0.3 eV.^{15,16} The observed transition energy of the midgap band was smaller than that of the CT band by 0.2 eV, which is almost consistent with the expectation.

In the spin-Peierls system with twofold degenerate ground states, nonlinear elementary excitations such as the polaron, spin soliton, and spin-0 soliton, are expected as shown in Fig. 1. In the case of DAP-TCNQ, the presence of the neutral site leads to the formation of the midgap state as described above. Taking account of the lattice dimerization, the midgap band is considered to originate from the polaron or spin-0 soliton. The polaron state is, however, excluded by comparing the oscillator strength of the midgap band with the remaining spin density below 100 K as follows: The total absorption intensity of the midgap band is about 30% of that of the CT band at 40 K as shown in Fig. 6. On the other hand the density of the remaining spin of DAP-TCNQ below 100 K is 9.2×10^{-4} per one site, estimated from the Curie contribution to the temperature dependence of the spin susceptibility. If the midgap state is related to an excitation with a spin, i.e., polaron, the oscillator strength of the midgap band needs to be 330 times larger than that of the CT band to explain the intensity of the midgap band; this factor is unreasonably large. Consequently the midgap band is considered to originate from the spin-0 soliton, which is a spinless domain wall between the A and B phase. [Fig. 1(c)] In the case of the midgap band of DAP-DMTCNQ, it is impossible to distinguish between the spin-0 soliton and the polaron by the spin density. However, it is considered that the midgap band is also due to the spin-0 soliton, since the experimental results observed in the present study were very similar to those of DAP-TCNQ.

A different assignment of the A and B bands may be possible; the A and B bands correspond to the CT transitions in the TCNQ and DAP columns, respectively, because of the different on-site Coulomb repulsion energy. However, this assignment appears to be inconsistent with the following experimental result: Only the intensity of the B band increases with decreasing temperature, while the A band was almost constant, as shown in Fig. 6. Since the temperature dependence of the intensity of the B band was similar to that of the a_g modes shown in Fig. 8, it is considered that the B band grows with lattice dimerization. On the other hand, the DAP and TCNQ columns dimerize simultaneously, shown by the activation of the a_g modes. If the A and B bands originate from the different stacks, both A and B bands should show similar temperature dependence in accordance with the lattice dimerization. Therefore it is concluded that the B band does not originate only from the DAP columns.

In the present system, the electron transfer from the occupied to the neutral site is expected to occur with the excitation energy, which may depend on the electron-lattice interaction. However, such a band was not observed in the reflectance spectrum above 0.1 eV. The transition energy of the band might be less than 0.1 eV.

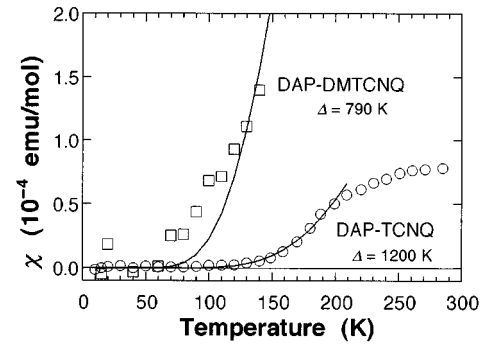


FIG. 11. Activation of the spin susceptibilities χ of DAP-TCNQ (open circles) and DAP-DMTCNQ (open squares) after subtracting the Curie contribution. The solid lines represent the fitting results of the data to Eq. (2). Δ is the spin-excitation energy.

Finally we will explain the activation of the midgap band due to the lattice dimerization from the viewpoint of the Hubbard model as follows: In the dimer with two electrons, the oscillator strength of the electron transfer is proportional to ta^2 ,³⁶ where a is the lattice constant. Since t is the overlap integral of the π orbitals, it is expected to be proportional to a^{-3} . Hence the oscillator strength and its change by the lattice distortion are proportional to a^{-1} and $-a^{-2}\delta a$, where δa is the lattice distortion. Since the midgap transition corresponds to the intradimer transition, the oscillator strength of the midgap state is enhanced with the larger amplitude of dimerization. On the other hand the oscillator strength of the CT band does not change much, since that of the interdimer transition decreases with dimerization at the same time.

C. DMTCNQ substitution effects

From the temperature dependence of the reflectance spectrum, the midgap absorption of DAP-DMTCNQ was found to be smaller than that of DAP-TCNQ at the same temperature, although the intensity of the CT band was almost the same as shown in Fig. 6. As discussed previously, the intensity of the midgap band becomes larger with the larger amplitude of the dimerization. Thus the lattice distortion in DAP-DMTCNQ is considered to be smaller than that in DAP-TCNQ at the same temperature. The difference in the amplitude of the dimerization between DAP-TCNQ and DAP-DMTCNQ is consistent with the results of IR spectroscopy, where the intensities of the a_g modes activated due to the dimerization are larger in DAP-TCNQ than those in DAP-DMTCNQ as shown in Fig. 8.

The magnetic property also shows the substitution effect. Figure 11 shows the activation of the spin susceptibility with temperature, which is obtained by subtracting the Curie component from the temperature dependence of the spin susceptibility. Since DAP-TCNQ and DAP-DMTCNQ are spin-Peierls systems, the spin-triplet state is formed by the thermal excitation beyond the magnetic gap. The activation energies of the magnetic susceptibilities of DAP-TCNQ and DAP-DMTCNQ below 200 K are estimated to be 1200 K (100 meV) and 790 K (68 meV), respectively. These energies were obtained from the temperature dependence of the spin susceptibility χ using the following expression:

$$\chi = (C/T)\exp(-\Delta/T), \quad (3)$$

where Δ is the activation energy, T is temperature, and C is a constant.³⁷ The fitting results are shown in Fig. 11 by the solid line. The smaller magnetic activation energy of DAP-DMTCNQ indicates the smaller lattice distortion by DMTCNQ substitution. Since the activation energy is proportional to $(\delta a)^{2/3}$ in the spin-Peierls system,³⁸ the estimated dimerization amplitude in DAP-TCNQ is 1.9 times larger than that in DAP-DMTCNQ.

In this way the substitution effects are attributable to the smaller lattice dimerization in DAP-DMTCNQ, which may be explained by the following: Firstly, it is found that the strength of the hydrogen bond formed between the DAP and DMTCNQ column is stronger than that of DAP-TCNQ, although it is not strong enough to lock the phase of dimerization as in the case of the *MX* compounds.^{5,6} This was shown by the larger frequency shift of the N-H stretching mode of the DAP molecule as described in Sec. IV C 2. The stronger hydrogen bond is expected to decrease the amplitude of the lattice distortion, which costs more elastic energy owing to the stronger interchain interaction, resulting in the larger modulus of elasticity along the stacking axis. This leads to the smaller dimerization in the spin-Peierls state. Secondly in the DMTCNQ column, the methyl group sticks out of the molecular plane in a DMTCNQ molecule, which would re-

sult in a stronger intermolecular repulsive interaction in the stack. Thus the same lattice distortion costs more elastic energy in the DMTCNQ column than in the TCNQ column, which also makes the dimerization small. These two correspond to the spin-lattice interaction becoming weaker by the substitution, indicating that the hydrogen bond is useful in modifying the electronic state of the spin-Peierls system.

VI. CONCLUSIONS

We have investigated the midgap state in the 1D spin-Peierls system, DAP-TCNQ and DAP-DMTCNQ. The band filling of the system slightly deviates from the half-filled regime, corresponding to the carrier injection. In the absorption spectrum, a midgap band, which is absent in the completely half-filled system, was found below the Hubbard gap. The midgap band is attributed to the spin-0 soliton, which is the neutral domain wall of the dimerized chains, taking account of the magnetic property. The amplitude of the lattice dimerization may be modified by the interchain hydrogen bond.

ACKNOWLEDGMENT

The authors would like to express their thanks to Dr. S. Hughes for a critical reading of the manuscript.

* Author to whom correspondence should be addressed.

¹A. J. Heeger, S. Kivelson, J. R. Schrieffer, and W. P. Su, *Rev. Mod. Phys.* **60**, 781 (1988).

²H. Endres, *Extended Linear Chain Compound*, edited by J. S. Miller (Plenum, New York, 1983), Vol. 3, Chap. 7.

³M. Imada, *Prog. Theor. Phys. Suppl.* **113**, 203 (1993).

⁴T. Inabe, K. Okaniwa, H. Ogata, H. Okamoto, T. Mitani, and Y. Maruyama, *Acta Chim. Hungarica-Models in Chem.* **130**, 537 (1993).

⁵H. Okamoto, K. Toriumi, T. Mitani, and M. Yamashita, *Phys. Rev. B* **42**, 10 381 (1990).

⁶H. Okamoto, T. Mitani, K. Toriumi, and M. Yamashita, *Mater. Sci. Eng. B* **13**, L9 (1992).

⁷T. J. Kistenmacher, T. J. Emge, A. N. Bloch, and D. O. Cowan, *Acta Crystallogr. B* **38**, 1193 (1982).

⁸J. F. Kwak, P. M. Chaikin, A. A. Russel, A. F. Garito, and A. J. Heeger, *Solid State Commun.* **16**, 729 (1975).

⁹P. M. Chaikin, R. L. Greene, S. Etemad, and E. M. Engler, *Phys. Rev. B* **13**, 1672 (1976).

¹⁰J. B. Torrance, B. A. Scott, and F. B. Kaufman, *Solid State Commun.* **17**, 1369 (1975).

¹¹J. B. Torrance, J. J. Mayerle, K. Bechgaard, B. D. Silverman, and Y. Tomkiewicz, *Phys. Rev. B* **22**, 4960 (1980).

¹²S. Matsuzaki, R. Kuwata, and K. Toyoda, *Solid State Commun.* **33**, 403 (1980).

¹³J. S. Chappell, A. N. Bloch, W. A. Bryden, M. Maxfield, T. O. Poehler, and D. O. Cowan, *J. Am. Chem. Soc.* **103**, 2442 (1981).

¹⁴D. B. Tanner, C. S. Jacobson, A. A. Bright, and A. J. Heeger, *Phys. Rev. B* **16**, 3283 (1977).

¹⁵K. Yakushi, T. Kusaka, and H. Kuroda, *Chem. Phys. Lett.* **68**, 139 (1979).

¹⁶K. Yakushi, S. Miyajima, T. Kusaka, and H. Kuroda, *Chem. Phys. Lett.* **114**, 168 (1985).

¹⁷H. Okamoto, Y. Tokura, and T. Koda, *Phys. Rev. B* **36**, 3858 (1987).

¹⁸M. J. Rice, *Phys. Rev. Lett.* **37**, 36 (1976).

¹⁹M. J. Rice, *Solid State Commun.* **31**, 93 (1979).

²⁰A. Painelli and A. Girlando, *J. Chem. Phys.* **84**, 5655 (1986).

²¹G. R. Anderson and J. P. Devlin, *J. Phys. Chem.* **79**, 1100 (1975).

²²Z. Iqbal, C. W. Christoe, and D. K. Dawson, *J. Chem. Phys.* **63**, 4485 (1975).

²³R. Bozio and C. Pecile, *J. Chem. Phys.* **67**, 3864 (1977).

²⁴M. J. Rice, V. M. Yartsev, and C. S. Jacobsen, *Phys. Rev. B* **21**, 3437 (1980).

²⁵S. Etemad, *Phys. Rev. B* **24**, 4959 (1981).

²⁶J. L. Musfeldt, K. Kamaras, and D. B. Tanner, *Phys. Rev. B* **45**, 10 197 (1992).

²⁷J. L. Musfeldt, C. C. Homes, M. Almeida, and D. B. Tanner, *Phys. Rev. B* **46**, 8777 (1992).

²⁸A. Girlando, F. Marzola, C. Pecile, and J. B. Torrance, *J. Chem. Phys.* **79**, 1075 (1983).

²⁹M. Meneghetti, A. Girlando, and C. Pecile, *J. Chem. Phys.* **83**, 3134 (1985).

³⁰Y. Tokura, H. Okamoto, T. Koda, T. Mitani, and G. Saito, *Solid State Commun.* **57**, 607 (1986).

³¹K. Okaniwa, H. Okamoto, T. Mitani, K. Toriumi, and M. Yamashita, *J. Phys. Soc. Jpn.* **60**, 997 (1991).

³²Y. Lepine, A. Caille, and V. Laroche, *Phys. Rev. B* **18**, 3585 (1978).

³³Y. Takaoka and K. Motizuki, *J. Phys. Soc. Jpn.* **47**, 1752 (1979).

³⁴Y. Lepine, *Phys. Rev. B* **28**, 2659 (1983).

³⁵S. Mazumdar and Z. G. Soos, *Phys. Rev. B* **23**, 2810 (1981).

³⁶C. S. Jacobsen, in *Semiconductor and Semimetals*, Vol. 27, edited by E. Conwell (Academic, Boston, 1988).

³⁷Y. Tomkiewicz, A. R. Taranko, and J. B. Torrance, *Phys. Rev. B* **15**, 1017 (1977).

³⁸M. C. Cross and D. S. Fisher, *Phys. Rev. B* **19**, 402 (1979).